

# Regulated Degradation of an Endoplasmic Reticulum Membrane Protein in a Tubular Lysosome in *Leishmania mexicana*

Kylie A. Mullin,<sup>\*†</sup> Bernardo J. Foth,<sup>†‡</sup> Steven C. Ilgoutz,<sup>\*</sup>  
Judy M. Callaghan,<sup>\*</sup> Jody L. Zawadzki,<sup>\*</sup> Geoffrey I. McFadden,<sup>†</sup>  
and Malcolm J. McConville<sup>\*§</sup>

<sup>\*</sup>Department of Biochemistry and Molecular Biology, and the Plant Cell Biology Research Centre,

<sup>†</sup>School of Botany, The University of Melbourne, Victoria 3010, Australia

Submitted November 22, 2000; Revised May 22, 2001; Accepted May 31, 2001

Monitoring Editor: Juan Bonifacino

The cell surface of the human parasite *Leishmania mexicana* is coated with glycosylphosphatidylinositol (GPI)-anchored macromolecules and free GPI glycolipids. We have investigated the intracellular trafficking of green fluorescent protein- and hemagglutinin-tagged forms of dolichol-phosphate-mannose synthase (DPMS), a key enzyme in GPI biosynthesis in *L. mexicana* promastigotes. These functionally active chimeras are found in the same subcompartment of the endoplasmic reticulum (ER) as endogenous DPMS but are degraded as logarithmically growing promastigotes reach stationary phase, coincident with the down-regulation of endogenous DPMS activity and GPI biosynthesis in these cells. We provide evidence that these chimeras are constitutively transported to and degraded in a novel multivesicular tubule (MVT) lysosome. This organelle is a terminal lysosome, which is labeled with the endocytic marker FM 4-64, contains lysosomal cysteine and serine proteases and is disrupted by lysomorphotropic agents. Electron microscopy and subcellular fractionation studies suggest that the DPMS chimeras are transported from the ER to the lumen of the MVT via the Golgi apparatus and a population of 200-nm multivesicular bodies. In contrast, soluble ER proteins are not detectably transported to the MVT lysosome in either log or stationary phase promastigotes. Finally, the increased degradation of the DPMS chimeras in stationary phase promastigotes coincides with an increase in the lytic capacity of the MVT lysosome and changes in the morphology of this organelle. We conclude that lysosomal degradation of DPMS may be important in regulating the cellular levels of this enzyme and the stage-dependent biosynthesis of the major surface glycolipids of these parasites.

## INTRODUCTION

Glycosylphosphatidylinositols (GPIs) glycolipids are used to anchor a diverse range of proteins to the plasma membrane in all eukaryotic cells and may also be abundant membrane components in their own right (Ferguson *et al.*, 1999; Tiede *et al.*, 1999; McConville and Menon, 2000). These glycolipids are assembled in the endoplasmic reticulum (ER) by the sequential transfer of monosaccharides and ethanolamine-phosphate to phosphatidylinositol and anchor precursors

subsequently transferred en bloc to the C terminus of proteins with a GPI signal sequence (Undenfriend and Kodukula, 1995). GPI biosynthesis is essential for the viability of yeast (Leidich *et al.*, 1994), some protozoa (Ilgoutz *et al.*, 1999a; Nagamune *et al.*, 2000), and mammalian embryogenesis (Nozaki *et al.*, 1999), and the synthesis of GPI anchor precursors appears to be tightly coupled to protein synthesis in the secretory pathway (Travers *et al.*, 2000). However, little is known about how enzymes involved in GPI biosynthesis and other ER glycosylation pathways are regulated during eukaryotic growth and development.

GPI biosynthesis is the major ER glycosylation pathway in many parasitic protozoa, including the sandfly-transmitted *Leishmania* spp. that cause a number of important diseases in humans (McConville and Ferguson, 1993; Ferguson *et al.*, 1999). The cell surfaces of these parasites are characteristically coated by GPI-anchored glycoproteins. In addition,

<sup>†</sup> These authors contributed equally to this work.

<sup>§</sup> Corresponding author. E-mail address: malcolmm@unimelb.edu.au. Abbreviations used: DPMS, dolichol-phosphate-mannose synthase; GPI, glycosylphosphatidylinositol; GFP, green fluorescent protein; LPG, lipophosphoglycan; MVB, multivesicular bodies; MVT, multivesicular tubule, PMSF, phenylmethylsulfonyl fluoride; TLCK, tosyl-lysylchloromethylketone.

*Leishmania* spp. synthesize an abundant GPI-anchored lipophosphoglycan (LPG) and a family of free GPIs that are the major glycolipids of these parasites (McConville and Blackwell, 1991; McConville and Ferguson, 1993; Mengeling *et al.*, 1997; Ilg *et al.*, 1999). These GPI-anchored macromolecules and free GPIs are most highly expressed in the promastigote (sandfly) stage and are thought to form a protective surface glycocalyx. They also mediate specific host-parasite interactions in the midgut of the sandfly vector and are required for promastigote invasion of macrophages in the mammalian host (Ilg, 2000; Sacks *et al.*, 2000; Spath *et al.*, 2000). Recent studies with the use of *L. mexicana* promastigotes suggest that the protein anchor and LPG anchor precursors and free GPIs are assembled on distinct phosphatidylinositol molecular species in a subcompartment of the ER (Ralton and McConville, 1998; Ilgoutz *et al.*, 1999b). Furthermore, they suggest that the biosynthesis of intermediates in these pathways is tightly regulated during parasite growth and differentiation. In particular, we have recently shown that the synthesis of all three GPI pools is markedly down-regulated as logarithmically growing promastigotes reach stationary phase, presumably reflecting a decreased requirement for membrane lipids in the latter stage (our unpublished results). Growth-dependent changes in GPI biosynthesis are also likely to account for the dramatic change in surface architecture of these parasites after promastigotes differentiate to amastigotes in the phagolysosome compartment of mammalian macrophages. Amastigotes lack the surface coat of GPI-anchored glycoproteins and LPG, but retain a densely packed surface layer of free GPIs that appear to be the major surface components (McConville and Blackwell, 1991; Bahr *et al.*, 1993; Winter *et al.*, 1994).

To further investigate the subcellular localization and growth-dependent changes in GPI biosynthesis in these parasites, we have expressed a green fluorescent protein (GFP) chimera containing functionally active dolichol-phosphate-mannose synthase (DPMS) in *L. mexicana* promastigotes (Ilgoutz *et al.*, 1999b). DPMS is a C-terminally anchored membrane protein that catalyzes the synthesis of dolichol-phosphate-mannose on the cytoplasmic leaflet of the ER. This sugar donor is rapidly used by three GPI-specific mannosyltransferases in the ER lumen (Ralton and McConville, 1998; Ilgoutz *et al.*, 1999a). Unexpectedly, the GFP-DPMS chimera primarily localized to a previously undescribed tubular compartment, rather than the bulk ER (Ilgoutz *et al.*, 1999b). This tubule extended from the flagellar pocket (a specialized invagination in the plasma membrane that surrounds the flagellum and the sole site of exo- and endocytosis in these parasites) toward the posterior end of the cell (Ilgoutz *et al.*, 1999b). We initially speculated that this organelle could correspond to the ER subcompartment detected in subcellular fractionation experiments. However, we now show that this organelle, termed the multivesicular tubule (MVT) (Mullin *et al.*, 2000; Weise *et al.*, 2000), is a terminal lysosomal compartment. Our data suggest that GFP-DPMS is correctly targeted to the same subcompartment of the ER as endogenous DPMS in logarithmically growing promastigotes, but is also constitutively transported to the MVT lysosome. In stationary phase promastigotes, essentially all of the GFP-DPMS chimera is transported to the MVT, coincident with a marked down-regulation in endogenous DPMS activity. These data suggest

that growth-dependent changes in the sorting and lysosomal turnover of ER glycosyltransferases in *L. mexicana* may play a role in regulating the synthesis of the major surface glycolipids of these parasites.

## MATERIALS AND METHODS

### Parasite Culture

Promastigotes of *L. mexicana* (strain MNYC/BZ/62/M379) were cultivated at 27°C in RPMI medium (Trace, Castle Hill, NSW, Australia) supplemented with 10% fetal bovine serum (Life Technologies, Gaithersburg, MD).

### DNA Constructs

Constructs encoding GFP, GFP-DPMS, and an ER signal sequence-GFP-MDDL fusion protein in the *Leishmania* expression vector pX (pGFP, pGFP-DPMS, and pGFP-MDDL, respectively) were generated as previously described (Ilgoutz *et al.*, 1999b). The following synthetic oligonucleotides (5' to 3') were used to generate a construct that encodes DPMS N-terminally tagged with three copies of the influenza hemagglutinin peptide epitope (pHA-DPMS). Nucleotides in bold denote sequence that was not complementary to the DNA template, but added to incorporate restriction endonucleases for cloning or to incorporate HA epitopes. The start codon is underlined and the stop codon is doubly underlined: primer 1, **GACTGGATCCATGTACCCGTACGACGTCCGGACTACGCCATGC** - **AGTACTCCATTATCG**, primer 2, **GATCGAATTCTAGACCT** - **AGAAGAGGGAATGGTAGAG**, primer 3, **TATCCCTATGATGTGCCGATTATGCGTACCCGTACGACGTCCCG**, primer 4, **GACTGGATCCATGTACCCGTACGACGTCCGGACTACGCTGCTGCTATCCCTATGATGTGCC**. A single HA-tagged DPMS amplicon was generated by polymerase chain reaction, with the use of primers 1 and 2 and a leishmanial DPMS genomic clone (Ilgoutz *et al.*, 1999a) as template. This amplicon was subsequently used as template for a second round of polymerase chain reaction with the use of primers 3 and 2, resulting in a double HA-tagged DPMS amplicon. A triple HA-tagged DPMS amplicon was then generated with the use of the double HA-tagged DPMS amplicon as template and primers 4 and 2. This amplicon was directionally cloned into the pX vector with the use of the restriction endonucleases *Bam*HI and *Xba*I. The N-terminal triple HA tag thus encoded the following sequence: MYPYDVPDYAGYPYDVPDYAYPYDVPDYA fused in frame with full-length DPMS. Plasmid DNA was prepared and parasites were transfected, as previously described (Ilgoutz *et al.*, 1999b).

### Fluorescence Microscopy

GFP chimeras were visualized in live *L. mexicana* promastigotes by confocal microscopy, as described previously (Ilgoutz *et al.*, 1999b). Briefly, promastigotes were pelleted by centrifugation (5000 × *g*, 10 s) and then resuspended in phosphate-buffered saline (PBS) containing concanavalin-A-TRITC (Sigma, St. Louis, MO) and 1% bovine serum albumin to label the cell surface glycocalyx and flagellar pocket. Endocytic and acidic compartments in live cells were also labeled by adding either FM 4-64 (8 μM from a 4 mM stock in dimethyl sulfoxide [DMSO]; Molecular Probes, Eugene, OR) or the acidotropic probe LysoTracker (50 nM; Molecular Probes) directly to the culture medium. Noninternalized FM 4-64 in the plasma membrane was back-extracted by resuspending promastigotes in fresh medium. Live promastigotes were immobilized for fluorescence microscopy by mounting under poly-L-lysine-coated coverslips. Samples were viewed with a Bio-Rad MRC1024 confocal scanning laser system installed on a Zeiss Axioplan II microscope with a krypton/argon laser as previously described (Ilgoutz *et al.*, 1999b). Images of 512 × 512 pixels were obtained with the use of Bio-Rad Lasersharp and processed with the use of Adobe Photo-

shop. For indirect immunofluorescence microscopy, *L. mexicana* promastigotes were fixed in 4% paraformaldehyde (15 min, on ice), washed in PBS, and then allowed to adhere to glass coverslips. The coverslips were sequentially incubated in methanol ( $-20^{\circ}\text{C}$ , 5 min), 50 mM  $\text{NH}_4\text{Cl}$ , and PBS containing 1% bovine serum albumin (PBS-BSA), and the adherent cells labeled with anti-HA antibody, 3F10 (1:40 dilution; Roche Molecular Biochemicals, Indianapolis, IN) in PBS-BSA for 30 min at  $25^{\circ}\text{C}$ . Coverslips were washed in PBS (3 times), before being immersed in Alexa-fluor<sup>TM</sup> 488 goat anti-rat IgG conjugate (1:200 dilution; Molecular Probes) in PBS-BSA for 30 min at  $25^{\circ}\text{C}$ . For double labeling experiments, the coverslips were washed with PBS (3 times) and then immersed in rabbit anti-BiP antiserum (1:100 dilution; provided by Dr J. Bangs; University of Wisconsin, Madison Medical School, Madison, WI) in PBS-BSA for 30 min at  $25^{\circ}\text{C}$ . Coverslips were washed with PBS (3 times) and then immersed in Texas Red goat anti-rabbit IgG conjugate (1:100 dilution; Jackson ImmunoResearch, West Grove, PA) in PBS-BSA (30 min,  $25^{\circ}\text{C}$ ). After washing in PBS (3 times), coverslips were mounted with Mowiol mounting medium for confocal microscopy as described above.

### Electron Microscopy

For electron microscopy, cells were fixed by adding a mixture of glutaraldehyde (25% stock, 7.1% final concentration) and osmium tetroxide (10% stock, ProSciTech, Thuringowa, Queensland, Australia; 1.2–1.6% final concentration) directly to mid-log phase cultures. After fixation at room temperature for 15 min, cells were gently collected by centrifugation ( $1000 \times g$ , 5 min) and washed three times with PBS. Cells were transferred to water in three steps, embedded in 1% agarose (DNA-grade; Progen, Darra, Queensland, Australia) and the agarose blocks dehydrated in a graded series of ethanol or acetone solutions (0–100% in 10% steps) on ice. Cells were embedded in LR Gold (ProSciTech) or Spurr's resin (after infiltration with propylene oxide), and ultrathin serial sections (80 nm) were mounted on pioloform-coated slot grids, poststained with aqueous uranyl acetate and lead citrate, and examined at 120 kV with the use of a Philips CM120 BioTWIN transmission electron microscope. For immunoelectron microscopy, cells were fixed with glutaraldehyde (7.1%) for 1 h on ice and then processed as described above for embedding in LR Gold. Ultrathin sections on slot grids were immersed in blocking buffer (PBS containing 0.8% bovine serum albumin and 0.01% Tween 80) for 30 min at room temperature and then incubated with a rabbit polyclonal anti-GFP antibody (1:300–1:500) in blocking buffer for 2–4 h at room temperature. After washing with blocking buffer, the sections were incubated with goat anti-rabbit antibodies (British BioCell International, Cardiff, United Kingdom) conjugated to 20-nm gold particles (1:20 dilution) for 16 h at  $4^{\circ}\text{C}$ . The sections were washed with blocking buffer, PBS, and water and poststained as described above.

### Analysis of Endogenous and Tagged Forms of DPMS

For analysis of endogenous DPMS activity, promastigotes were solubilized in 50 mM HEPES-NaOH pH 7.5, 2 mM EGTA, 5 mM  $\text{MgCl}_2$ , 2.5 mM dithiothreitol (DTT), 1 mM ATP, 0.2 mM tosyllysylchloromethylketone (TLCK), 2  $\mu\text{M}$  leupeptin, 0.1 mM phenylmethylsulfonyl fluoride (PMSF), and 0.4% Triton X-100 for 10 min at  $0^{\circ}\text{C}$ . The total extract containing  $10^6$  cell equivalents was diluted in 50  $\mu\text{l}$  of the same buffer containing 75  $\mu\text{M}$  dolichol-phosphate (C40-C65) and 0.3 mM GDP- $^3\text{H}$ Man (0.3  $\mu\text{Ci}$ ) and incubated for 40 min at  $15^{\circ}\text{C}$  (Ilgoutz *et al.*, 1999b). The reaction was stopped by addition of 2 volumes of water-saturated 1-butanol and radioactivity in the upper 1-butanol phase quantitated by scintillation counting. Levels of expression of the GFP- and HA-tagged DPMS were quantitated by Western blotting. Promastigotes were extracted in chloroform/methanol/water and precipitated proteins analyzed by SDS-PAGE. Protein was transferred to nitrocellulose and the blots probed with anti-GFP (1:1000 dilution; Roche Molecular Biochemi-

cal), anti-HA (1:200 dilution; Roche Molecular Biochemicals), or anti-*T. brucei* BiP (1:5000 dilution) (Bangs *et al.*, 1993) antibodies. The blots were subsequently probed with either anti-mouse or anti-rabbit antibody-horseradish peroxidase conjugate (1:10,000; Bio-Rad, Richmond, CA), respectively, and bands detected by enhanced chemiluminescence (Amersham Pharmacia Biotech, Arlington Heights, IL) according to the manufacturer's instructions.

### Subcellular Fractionation

*Leishmania mexicana* promastigotes were hypotonically lysed and microsomes in the 3000-g supernatant were fractionated by isopycnic centrifugation on a 15–60% sucrose gradient (Ilgoutz *et al.*, 1999b). BiP (a general ER marker) was detected by SDS-PAGE and quantitative immunoblotting. DPMS (ER subcompartment) was assayed as previously described (Ilgoutz *et al.*, 1999b). Protease activity was measured with the use of substrate SDS-PAGE (Brooks *et al.*, 2000). Briefly, fractions from the sucrose gradient were preincubated in 50 mM sodium acetate buffer, pH 5.5 (30 min,  $27^{\circ}\text{C}$ ) and protein concentrated by solvent precipitation. Samples were resuspended in reducing sample buffer (without heating) and electrophoretically resolved under reducing conditions in 12% (wt/vol) acrylamide gels incorporating 0.2% (wt/vol) gelatin, run under reducing conditions. The gels were washed sequentially with 0.25% (vol/vol) Triton X-100 and 0.1 M sodium acetate buffer, pH 5.5, containing 1 mM DTT to reconstitute protease activity and then incubated in 0.1 M sodium acetate, pH 5.5, 1 mM DTT for 12 h at  $25^{\circ}\text{C}$ . The location of proteases was detected by staining with 0.25% Coomassie Blue R-250 (Brooks *et al.*, 2000).

### Treatment with Lysosome-disrupting Compounds

*L. mexicana* promastigotes expressing the GFP-DPMS chimera were incubated in RPMI-10% fetal bovine serum at  $27^{\circ}\text{C}$  in the presence of either 250 nM bafilomycin  $\text{A}_1$ , 20  $\mu\text{M}$  monensin, or 80  $\mu\text{M}$  imipramine. These compounds were made up as stock solutions in DMSO or ethanol and diluted to give a final concentration of 0.5% DMSO or ethanol. Control incubations were performed in the presence of the equivalent amounts of DMSO or ethanol.

### Cell Surface Labeling and Transport of gp63

The surface transport of the major surface glycoprotein gp63 was monitored by surface biotinylation. Mid-log growth promastigotes ( $6 \times 10^6$  cell/ml) were incubated in conditioned medium containing either 250 nM bafilomycin  $\text{A}_1$  or 0.3% DMSO for 1 h at  $27^{\circ}\text{C}$ . Cells were washed and suspended at  $2 \times 10^8$  cells/ml in methionine-free RPMI medium containing 1% bovine serum albumin with or without bafilomycin  $\text{A}_1$  (20 min at  $27^{\circ}\text{C}$ ) and then pulse-labeled for 5 min with  $^3\text{S}$  Trans-label (100  $\mu\text{Ci}$ /ml; ICN, Costa Mesa, CA). The cells were centrifuged ( $3000 \times g$ , 30 s) and suspended at  $2 \times 10^7$  cell/ml in complete RPMI-10% fetal bovine serum with or without 250 nM bafilomycin  $\text{A}_1$ . After a 2-h chase, cells were washed with ice-cold biotinylation buffer (10 mM triethanolamine pH 8.5, 2 mM  $\text{CaCl}_2$ , 0.25 M sucrose, 10 mM glucose) and then resuspended in biotinylation buffer containing 1.5 mg/ml NHS-SS-biotin (Sigma) for 30 min at  $4^{\circ}\text{C}$ . Cells were washed with PBS, pH 8.5, containing 100 mM glycine and solubilized in PBS containing 1% Triton X-114, 0.2 mM TLCK, 0.2  $\mu\text{M}$  leupeptin, and 0.1 mM PMSF. After recovery of GPI-anchored proteins by temperature-induced phase separation (Bordier, 1981), the detergent-enriched phase was diluted to 1% Triton X-114 in PBS and incubated with 30  $\mu\text{l}$  of packed streptavidin-agarose beads (Sigma) overnight at  $4^{\circ}\text{C}$  with gentle agitation. The beads were centrifuged and the supernatant (unbound fraction) retained. The beads were sequentially washed with 10 mM Tris-HCl, pH 7.4, containing 1) 0.5 M NaCl, 1 mM EDTA, 1% NP-40; 2) 0.15 M NaCl, 1 mM EDTA, 1% NP-40, 0.1% SDS; and 3) 0.1% NP-40 and then boiled in PBS containing 50 mM DTT, 0.2% SDS to release protein bound to the beads by the biotin disulfide linker. Protein in

the bound and unbound fractions were precipitated in 90% ice-cold acetone and analyzed by SDS-PAGE. Labeled proteins were detected by fluorography in Amplify (Amersham Pharmacia Biotech) and bands quantitated by densitometry.

### Proteolytic Degradation of GFP

*L. mexicana* promastigotes expressing the GFP-DPMS chimera were harvested at either log ( $8 \times 10^6$  cells/ml) or stationary ( $1.4 \times 10^7$  cells/ml) growth and incubated in conditioned RPMI-10% fetal bovine serum with or without protease inhibitors (10  $\mu$ M E64d, or 0.1 mM PMSF and 10 mM DTT) for 30 min at 27°C. Cells were washed in PBS and suspended in either 50 mM Tris-HCl pH 7.5, 100 mM NaCl, 1 mM EDTA (pH 7.5 medium) or 50 mM acetate buffer pH 5.5, 100 mM NaCl, 1 mM EDTA (pH 5.5 medium), with or without protease inhibitors for 2 h at 27°C. Proteins were precipitated and analyzed by SDS-PAGE and immunoblotting with anti-GFP antibody as described above. In some experiments, cells were preincubated in RPMI medium containing 250  $\mu$ M cycloheximide.

## RESULTS

### Down-Regulation of DPMS and Degradation of Epitope-tagged Forms of DPMS in Log and Stationary Phase *L. mexicana* Promastigotes

We have recently shown that the rate of synthesis of free GPIs and the GPI-anchored LPG decreases dramatically as logarithmically growing *L. mexicana* promastigotes reach stationary growth (our unpublished results). To examine whether decreased GPI biosynthesis in stationary phase cells is associated with the down-regulation of specific GPI enzymes, the activity of DPMS, a key enzyme in GPI biosynthesis, was measured in log, late log, and stationary phase cultures. As shown in Figure 1A, the cellular levels of DPMS activity decreased markedly as log phase promastigotes reached stationary growth. Because posttranscriptional and posttranslational mechanisms are thought to be important in regulating the cellular levels of many proteins in these parasites, we next investigated whether the low levels of DPMS activity in stationary phase cultures were due to increased degradation of this enzyme. A fusion construct of DPMS containing a triple HA epitope tag at the amino terminus (HA-DPMS) was constitutively expressed from the pX episome in *L. mexicana* promastigotes. This epitope-tagged protein was readily detected in logarithmically growing promastigotes (Figure 1B) and was localized to the nuclear envelope and peripheral ER by indirect immunofluorescence (Figure 2A). Interestingly, the distribution of the HA-DPMS overlapped with, but was not coincident with staining for the endogenous luminal ER marker BiP (Figure 2, B and C), consistent with our previous finding that the endogenous DPMS is present in a subcompartment of the ER [Ilgoutz *et al.*, 1999b]. In contrast, the HA-DPMS protein could not be detected by either Western blotting (Figure 1B) or indirect immunofluorescence (our unpublished results) in stationary phase promastigotes. The down-regulation of this protein was not due to decreased expression from the pX episome as levels of another ER-localized GFP chimera, GFP-MDDL (containing an N-terminal signal sequence and C-terminal ER retention signal [Bangs *et al.*, 1993]) was expressed in the ER at similar levels in both log and stationary phase promastigotes (Figure 2, H and I). Moreover, the endogenous marker BiP was also expressed at similar levels in log and stationary phase cells (Figure 1B), suggesting that

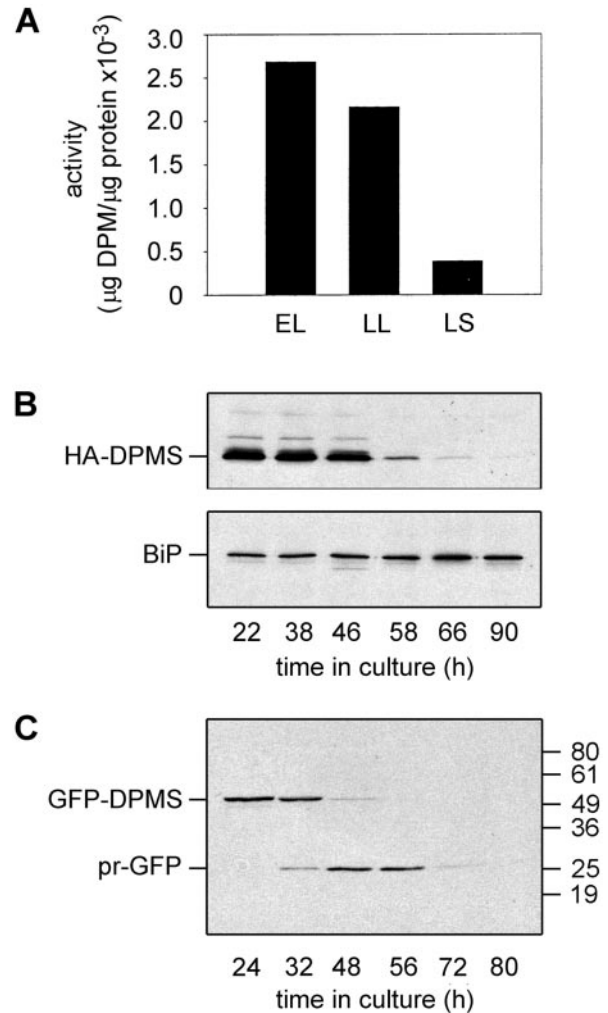


**Figure 1.** Down-regulation of DPMS and degradation of tagged DPMS. (A) Cellular levels of DPMS activity were measured in early log (EL), late log (LL), and late stationary phase (LS) cells. (B) Steady-state levels of HA-tagged DPMS and the luminal ER marker BiP were detected by Western blotting of protein extracted from  $10^6$  cell equivalents taken at different times in the growth curve. The down-regulation of endogenous DPMS activity correlates with the degradation of HA-tagged DPMS, whereas cellular pools of BiP remain constant. (C) Steady-state levels of the GFP-DPMS chimera and its degradation to a 25-kDa band, pr-GFP, was monitored by Western blotting.

the degradation of HA-DPMS was not due to the general autophagic degradation of the ER. These data show that HA-DPMS is primarily expressed in the ER in log phase promastigotes and indicate that constitutively expressed forms of DPMS are efficiently degraded in stationary phase cells.

### Degradation of GFP-DPMS Is Associated with Transport from ER to a Novel Tubular Organelle

We have previously shown that expression of a functionally active GFP chimera of DPMS in *L. mexicana* promastigotes

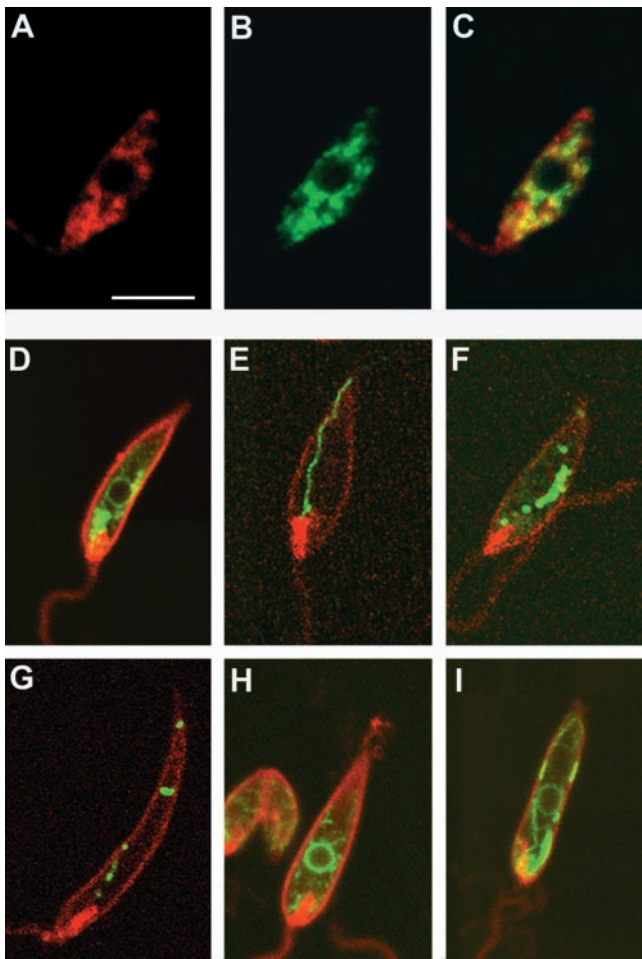


**Figure 2.** The GFP-DPMS chimera redistributes from the ER to a novel tubular compartment when *L. mexicana* promastigotes reach stationary growth. Confocal scanning microscopy of *L. mexicana* promastigotes. (A–C) *L. mexicana* promastigotes expressing HA-DPMS were harvested in log phase and fixed in paraformaldehyde. Fixed promastigotes were double labeled with anti-HA (A, red) and anti-BiP (B, green) antibodies. Merged images (C) show that HA-DPMS has an overlapping distribution with BiP in the ER of log phase promastigotes. (D–I) *L. mexicana* promastigotes expressing the GFP-DPMS were harvested in early log (D), late log (E), stationary (F), and late stationary (G) phases. Promastigotes were prelabeled with concanavalin-A-TRITC (red, to label cell surface and flagellar pocket) before the GFP fluorescence (green) was visualized in live cells. (H and I) *L. mexicana* promastigotes expressing GFP-MDDL (containing an N-terminal signal sequence and C-terminal ER retention motif) were harvested in log (H) and stationary phase (I). Promastigotes were prestained with concanavalin-A-TRITC as described above. Bar, 5  $\mu\text{m}$ .

results in the accumulation of GFP fluorescence in a novel tubular organelle rather than the ER (Ilgoutz *et al.*, 1999b). To investigate whether this compartment is associated with the degradation of DPMS chimeras we examined whether the GFP-DPMS chimera was also degraded in a growth-dependent manner and whether this degradation was associated with a change in the subcellular distribution of this chimera in live cells. As shown in Figure 1C, the full-length GFP-

DPMS chimera was degraded as logarithmically growing promastigotes reached stationary phase with essentially the same kinetics as the HA-DPMS (Figure 1B). However, the degradation of the GFP-DPMS chimera was associated with the appearance of a 25-kDa protein that accumulated during log growth and was gradually degraded after disappearance of the full-length chimera in stationary phase cells (Figure 1C). This protein was recognized by the anti-GFP antibodies and was slightly smaller than the native, cytosolic form of GFP (27 kDa). It was also quantitatively released from sonicated cells and was fluorescent when analyzed by native gel electrophoresis (our unpublished results), suggesting that it corresponds to the soluble, protease resistant GFP moiety (pr-GFP) of the GFP-DPMS chimera.

The growth-dependent degradation of the GFP-DPMS chimera was associated with a marked change in the subcellular distribution of GFP fluorescence in live parasites. In early log phase cells, the majority of the GFP fluorescence was localized to the ER, as shown by staining of both the nuclear envelope and the cortical reticulum (Figure 2D). However, in late log phase cells, GFP fluorescence was predominantly associated with the previously described tubular organelle that invariably extended from a region near the flagellar pocket toward the posterior end of the promastigote (Figure 2E) (Ilgoutz *et al.*, 1999b). This tubule characteristically fragmented into a series of vesicles in stationary phase cells (Figure 2F). By day 4, when promastigotes had assumed the elongated cell shape of metacyclic promastigotes, the GFP chimera was not detected by immunoblotting (Figure 1C) and was restricted to a few isolated vesicles when live parasites were examined by confocal fluorescence microscopy (Figure 2G). In contrast, a soluble GFP-MDDL chimera (Figure 2, H and I) and the endogenous BiP (our unpublished results) could be readily detected in the ER in both log and stationary phase cells. These results indicate that the degradation of GFP-DPMS is associated with the accumulation of GFP fluorescence in the tubule and associated structures and provide the first line of evidence that this compartment may be a degradative compartment.

#### ***GFP-DPMS and pr-GFP Are Present in Distinct Subcellular Compartments***

To examine whether the GFP-DPMS chimera was being degraded in the ER, a crude extract of *L. mexicana* promastigotes membranes was fractionated by isopycnic centrifugation on a 15–60% sucrose density gradient. As shown previously, the luminal ER marker BiP is distributed across the gradient as two broad peaks (Figure 3A; Ilgoutz *et al.*, 1999b). In contrast, DPMS (Figure 3A) and other GPI enzymes (Ilgoutz *et al.*, 1999b) are associated with BiP-containing fractions near the top of the gradient, which may represent a subcompartment of the ER (Ilgoutz *et al.*, 1999b). The intact GFP-DPMS chimera cosedimented with DPMS activity, suggesting that this chimera was being correctly targeted within the ER (Figure 3A). In contrast, the pr-GFP degradation product cosedimented with the major lysosomal markers near the bottom (fractions 11–14) and at the top (fractions 1–3) of the gradient (Figure 3A). The pr-GFP and cysteine proteases at the top of the gradient (fractions 1–3) were not associated with sedimentable membranes (our unpublished results), suggesting that they had been released from an intracellular luminal compartment during cell lysis. In sup-

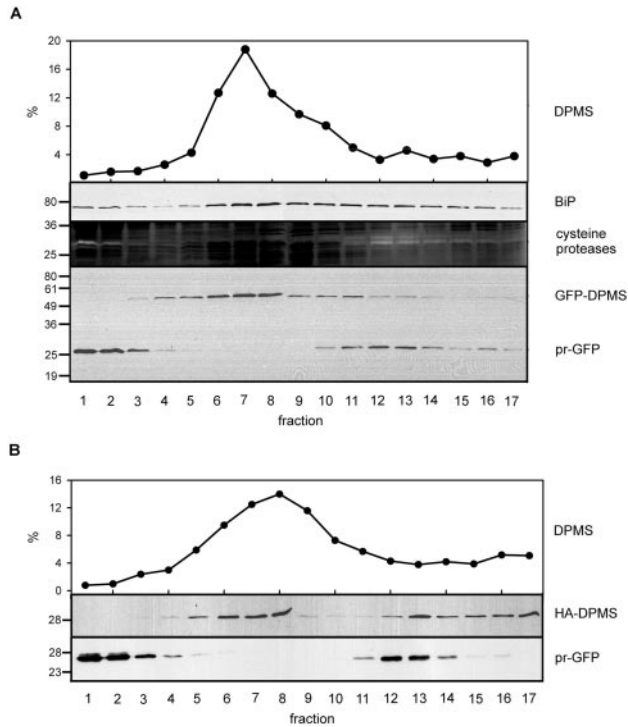


**Figure 3.** Localization of intact and degraded forms of GFP-DPMS to the ER and lysosomes, respectively. *L. mexicana* promastigotes expressing GFP-DPMS or HA-DPMS were hypotonically lysed and the crude cell extract in a 3000-g supernatant subjected to isopycnic fractionation on a 15–60% sucrose density gradient. (A) Mid-log promastigotes expressing GFP-DPMS. (B) Equal numbers of mid-log promastigotes expressing GFP-DPMS and HA-DPMS were mixed and the combined crude cell extracts analyzed on the same sucrose gradient. Fractions were assayed for DPMS (light ER) and cysteine proteases (lysosomes) by enzymatic assay and substrate SDS-PAGE, respectively. BiP (bulk ER), GFP-DPMS, and HA-DPMS were assayed after SDS-PAGE and Western blotting. GFP-DPMS was found in the same fractions as endogenous DPMS (fractions 6–8). The pr-GFP breakdown product was present in dense fractions containing lysosomal markers (fractions 11–13) or at the top of the gradient with cytosolic and released lysosomal proteins (fractions 1–3). The HA-DPMS was found in both the light ER and dense lysosomal fractions that peaked with pr-GFP in the same gradient. Sucrose concentrations increase from left to right in the figure.

port of this conclusion, GFP was never detected in the cytosol by fluorescence microscopy (Figure 2, D and E), although both pools of pr-GFP were fluorescent when analyzed on nonreducing polyacrylamide gels (our unpublished results) or by immuno-EM (Figure 4). These results suggest that the intact GFP-DPMS is correctly targeted to the same membranes as endogenous DPMS and that the pr-GFP degradation product is present in a distinct compartment, most likely the tubule, which contains lysosomal proteases.

Interestingly, some of the GFP-DPMS overlapped with the pr-GFP-containing fractions, suggesting that this chimera may reach the tubule before being degraded. To examine whether other forms of DPMS are present in these fractions, we investigated the subcellular distribution of HA-DPMS in sucrose gradients. As expected, most of the HA-DPMS co-

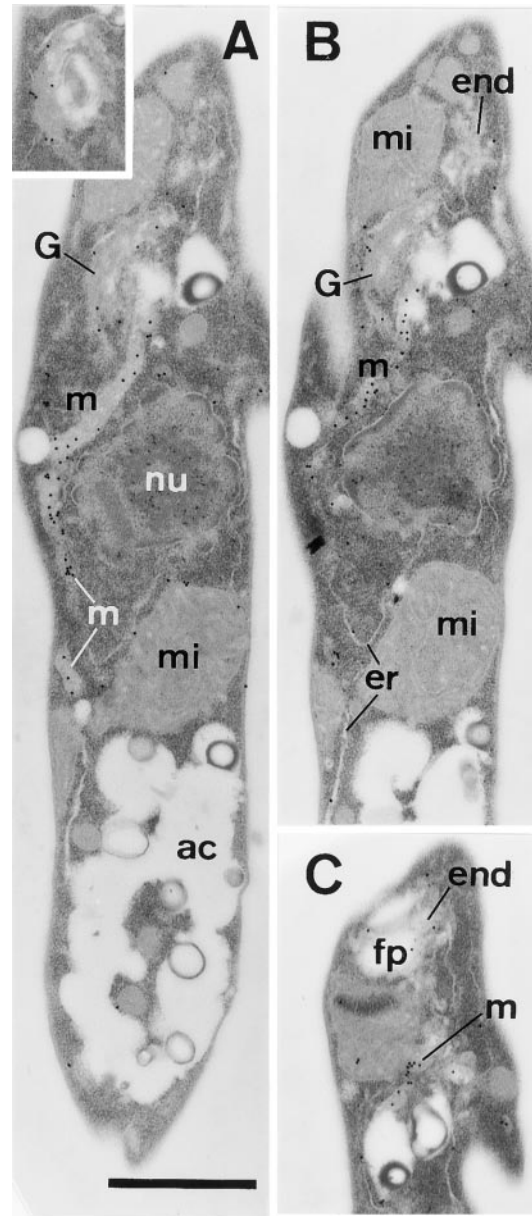


**Figure 4.** Immuno-EM localization of GFP to the ER and tubule. *L. mexicana* promastigotes expressing the GFP-DPMS chimera were fixed in glutaraldehyde and sections probed with anti-GFP polyclonal antibody followed by 20-nm gold-labeled secondary antibody. (A–C) represent serial sections from the same cell. (A) Longitudinal section of *L. mexicana* promastigote showing gold labeling of a continuous tubule that extends from the single anteriorly located Golgi apparatus, past the nucleus, toward the posterior end of the cell. Label is primarily across the lumen of the tubule. Gold particles are also present on the nuclear envelope and across the Golgi apparatus. No label is present on the acidocalcisomes. (Insert) Previous serial section (–2 from section in A) showing label over the *cis*-Golgi/transitional ER. (B) Serial section (+1 from section in A) of anterior end of cell confirming the tubular nature of the gold-labeled organelle. (C) Serial section (+4 from section in A) showing gold labeling of the tubule and endosomes near the flagellar pocket. Acidocalcisome (ac), endoplasmic reticulum (er), flagellar pocket (fp), Golgi apparatus (G), multivesicular tubule (m), nucleus (nu), tubular-vesicular network/endosome (t). Bar, 1  $\mu$ m.

sedimented with endogenous DPMS (Figure 3B, fractions 6–8). However, a minor but significant pool of HA-DPMS overlapped with the pr-GFP band near the bottom of the gradient (Figure 3B, fractions 12–14). Significantly, these fractions were not associated with a peak of DPMS activity, suggesting that this second pool of HA-DPMS is not functionally active. The distribution of HA-DPMS was also distinct from that of BiP (Figure 3A). Collectively, these data suggest that membrane-anchored forms of DPMS can be transported to the tubule before they are degraded.

### ***Tubule Compartment Is a Multivesicular, post-Golgi Compartment***

To further define the function of the tubule and its relationship to other organelles in the secretory pathway, wild-type and GFP-DPMS expressing *L. mexicana* promastigotes were fixed in mid-log phase and analyzed by electron microscopy (EM). When sections from fixed cells were stained with the anti-GFP antibody and gold-labeled secondary antibody, a prominent tubular organelle was labeled, which invariably extended from a region near the *trans*-face of the single anteriorly located Golgi apparatus, toward the posterior end of the cell (Figure 4, A and B). The tubular nature of this organelle was confirmed by serial sectioning (Figure 4, A–C). In all sections, the gold label over the tubule was primarily or exclusively found over the lumen, rather than in the limiting membrane of this organelle (Figure 4, A and B). Gold label was also associated with the nuclear envelope and other regions of the ER, as well as with the both the *cis*- and *trans*-face of the Golgi apparatus (Figure 4A and insert). Some label was also detected over a population of tubular-vesicular endosomes near the flagellar pocket (Figure 4C). In contrast, the mitochondrion and the large vacuolar acidocalcisomes at the posterior end of the promastigote were not labeled (Figure 4A).

To define more precisely the ultrastructure of the labeled organelles and their relationship with other organelles at the anterior end of the cell, promastigotes were fixed in glutaraldehyde/OsO<sub>4</sub>. This fixation procedure resulted in the preservation of a prominent MVT that extended from a region proximal to the flagellar pocket to the extreme posterior end of some cells (m in Figure 5, A–E, and H). This organelle has a diameter of ~60–120 nm and contains many membrane-bound ~30-nm intraluminal vesicles (Figure 5F). The MVT was often closely associated with either one or two cytoplasmic microtubules that are clearly distinct from the subpellicular microtubules that underlie the plasma membrane (Figures 5, C and D, and 6A). These microtubules appear to become intercalated into the subpellicular array at the posterior end of the cell (Figure 5C). We were unable to confirm whether they are continuous with the microtubule quartet that originates at the flagellar basal body and extends up the side of the flagellar pocket membrane (Figure 6D). In many cells, the MVT was only apparent as a series of discrete multivesicular bodies (MVBs) or short tubules in single sections (Figure 6, A–C). However, consecutive serial sections showed that these bodies were usually part of a continuous structure that extended from near the Golgi apparatus to the posterior end of the cell (our unpublished results). It is thus likely that both the continuous and discontinuous multivesicular structures seen in fixed cells are part of the continuous tubular structure seen in live trans-

ected cells expressing the GFP-DPMS chimera (Figure 2E) or wild-type cells labeled with the fluorescent lipid analog BODIPY-ceramide (Ilgoutz *et al.*, 1999b). Interestingly, in some sections the MVT appeared to be closely associated with extensions of the mitochondrion (Figure 5G), as previously observed by fluorescence microscopy (Ilgoutz *et al.*, 1999b).

In addition to the MVT, a distinct class of MVBs with the same internal structure as the MVT was commonly present near the anterior end of the MVT (v in Figure 5B) and proximal to the *trans*-face of the Golgi apparatus (Figure 7, C–F). The single, anteriorly located Golgi apparatus typically contained five or six stacked cisternae, and could be readily orientated by the presence of a prominent transitional ER (tER) along the *cis* (posterior)-face of the stack in serial sections (Figure 7A and C–F). The space between the tER (a cisternal extension of the cortical ER) and the *cis*-face of the Golgi was typically full of 30–50-nm vesicles (Figure 7, C–F), suggesting that this is the primary site of vesicular transport between the ER and the Golgi apparatus. Similar vesicles were also found around the lateral margins of the Golgi cisternae. In contrast, a number of morphologically distinct vesicles were evident at the *trans*-face of the Golgi stack, which appeared to be the equivalent of the TGN in other eukaryotes. These included small 30–50-nm vesicles (similar to those found in other parts of the Golgi apparatus), large translucent vesicles or saccules (80–500 nm in width) of varying shape, and a population of uniform ~230-nm-diameter MVBs, which were identical to those seen near the anterior end of the MVT (Figure 5, D–F). Serial sectioning revealed that several MVBs were associated with the *trans*-cisternae of the Golgi complex (Figure 7, D–F). The small vesicles and large polymorphic vesicles/saccules were often found anterior to the Golgi apparatus, juxtaposed to the flagellar pocket membrane. In contrast, the MVBs were never observed to lie directly next to the flagellar pocket membrane (Figure 5, B and C). These MVBs may thus act as a separate compartment and/or transport intermediates between the Golgi apparatus and the MVT (Figure 5H). Collectively, these studies suggest that the MVBs and MVT are post-Golgi compartments and that they have the characteristic internal structure of late endosomes or lysosomes (Grubenberg and Maxfield, 1995; Odorizzi *et al.*, 1998).

### ***Transport of Styryl Dye FM 4-64 into MVT***

To determine whether the MVT represents an intermediate endosomal or terminal lysosomal compartment *L. mexicana* promastigotes were stained with the nonexchangeable styryl dye FM 4-64, which is commonly used as a nonselective marker of endocytic pathway (Vida and Emr, 1995). FM 4-64 was rapidly incorporated into the plasma membrane and flagellar pocket (Figure 8A) and subsequently internalized after 10–20 min into a network of membranes surrounding the flagellar pocket at 27°C (Figure 8, C and D). These membranes have a tubular-vesicular structure (our unpublished results) and are the leishmanial equivalent of (early) endosomes (Wiese *et al.*, 1996, 2000). FM 4-64 was subsequently transported to a tubular structure with the same morphology as the MVT between 30 and 120 min (Figure 8E). When cells expressing the GFP-DPMS chimera were labeled with FM 4-64 for 2 h, the dye was found to colocalize exactly with GFP in the MVT (Figure 8, F–F'). Uptake of FM

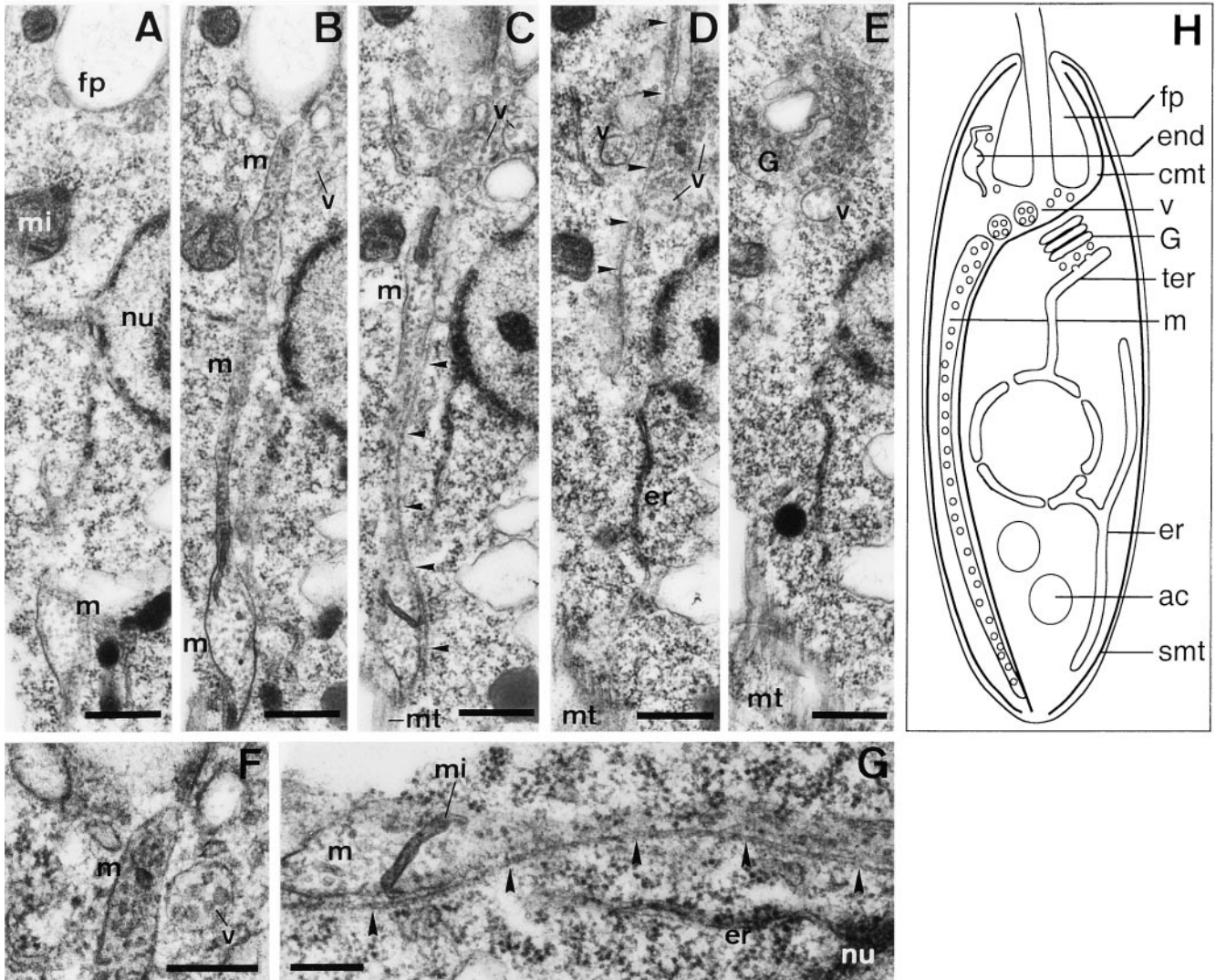


**Figure 5.** Ultrastructure of the MVT. (A–E) Consecutive 80-nm serial sections of glutaraldehyde/OsO<sub>4</sub>-fixed *L. mexicana* promastigotes. The sections show the longitudinal axis of the cell with the flagellar pocket at the top (fp) and the nucleus in the middle of the cell. The Golgi apparatus can be seen in E (across the plane of the *trans*-cisternae). A prominent MVT (m) can be seen running down the side of the nucleus in two of the sections (B and C). In addition, this series shows the presence of many multivesicular bodies between the anterior end of the MVT and the Golgi apparatus (B–E; detail of B in F), the presence of one or more cytoplasmic microtubules (arrows; detail of C in G) extending along the length of the MVT (these microtubules originate near the flagellar pocket and may become intercalated into the subpellicular microtubule cytoskeleton near the posterior end of the cell) (B and C) and the presence of mitochondria profiles closely associated with the MVT (G and C). (H) Schematic representation of secretory and endocytic organelles in exponentially growing *L. mexicana* promastigotes. Acidocalcisomes (ac), endoplasmic reticulum (er), flagellar pocket (fp), Golgi apparatus (G), multivesicular tubule (m), mitochondrion (mi), cytoplasmic microtubules (arrows in A–G; cmt in H), subpellicular microtubules (mt in A–E, smt in H), nucleus (nu), multivesicular bodies (v). Bars, 400 nm (A–E) and 200 nm (F and G).

4-64 was completely inhibited at 4°C (Figure 8B), whereas transport from the early endosomes to the MVT was selectively inhibited at 10°C (Figure 8, G–G’). Interestingly, the labeling of both the early endosomes and the MVT was relatively stable even after long (12 h) chase periods (our unpublished data), suggesting this dye may be continuously cycling between these two membrane compartments.

In contrast, the MVT was not detectably labeled with the acidotropic dye LysoTracker (Figure 8H), suggesting that it

does not contain a highly acidic lumen. However, LysoTracker strongly stained the large vacuolar acidocalcisomes at the posterior end of the promastigotes (Figures 4A, 7B, and 8H). These acidified vacuoles contain calcium and polyphosphate stores and lack lysosomal hydrolases (Do-campo and Moreno, 1999). The acidocalcisomes characteristically contained a homogeneous, electron dense lumen (even without uranyl and lead poststaining), which in some cases was leached out during fixation (Figures 4A and 7B).

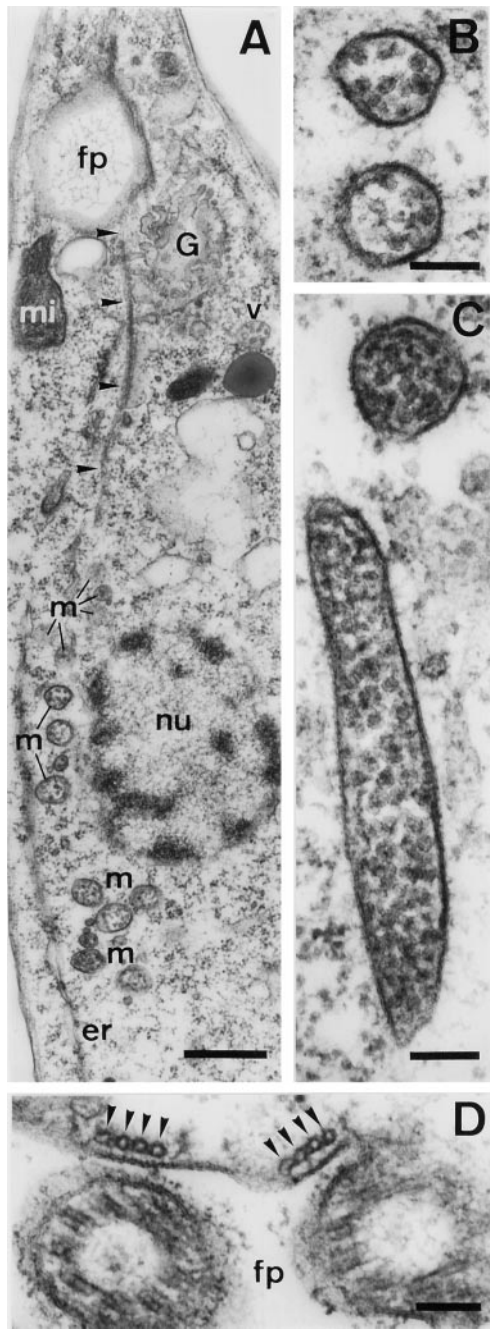


**Figure 6.** Detail of the MVT and cytoplasmic microtubules. (A–C) In many cells, the MVT appears as a series of distinct vesicles and short tubules (presumably due to vesicularization of the MVT during fixation) that contain many intraluminal vesicles. A linear alignment of these vesicles and tubules along the longitudinal axis of the cell is clearly evident, especially from observations made on serial sections (our unpublished results). One or two cytoplasmic microtubules (arrows) commonly flank the vesicles and tubules comprising the MVT. (D) Two sets of four specialized microtubules (arrows) that line the flagellar pocket membrane in a dividing cell. The membrane just subtending a microtubule quartet appears more electron dense than the remainder of the flagellar pocket membrane. Abbreviations are as described in Figure 4. Bars, 500 nm (A) and 100 nm (B–D).

Significantly, FM 4-64 was never seen to accumulate in these organelles consistent with the notion that they are not connected to the endosomes or lysosomes by vesicular transport. Taken together, these results suggest that the MVT is the terminal compartment in the endocytic pathway and that it is weakly acidic compared with the acidocalcisomes.

### *MVT Structure Is Perturbed by Lysomorphotropic Agents*

We next investigated whether these compartments were affected by alkalinizing agents known to perturb endosome/lysosome function. Incubation of *L. mexicana* promastigotes with 250 nM bafilomycin A<sub>1</sub>, a specific inhibitor of vacuolar-type H<sup>+</sup>-ATPases, resulted in the dramatic collapse of the MVT to one or two large vesicles within 30 s (Figure 8I). This collapse was extremely rapid, suggesting that the MVT is under elastic tension. In contrast, the structure of the ER stained with GFP-MDDL was unchanged by bafilomycin A<sub>1</sub> treatment (our unpublished results). Essentially identical results were obtained when cells were incubated instead with either monensin, a Na<sup>+</sup>/H<sup>+</sup> exchanger, or imipramine, a membrane-permeant amine (our unpublished results), suggesting that the maintenance of pH gradients across the MVT membrane or other intracellular pH gradients is required for MVT structure.

### *An Intact MVT Is Not Required for Anterograde Surface Transport of GPI-anchored Glycoproteins*

To discount the possibility that the MVT may be part of the secretory pathway, we investigated whether perturbation of MVT structure affected the secretory transport of the major surface glycoprotein gp63/leishmanolysin. Surface transport of gp63 was measured by pulse/chase labeling cells with [<sup>35</sup>S]methionine and surface biotinylation. gp63 was transported to the cell surface with a lag of ~15 min and a *t*<sub>1/2</sub> of 50 min in untreated cells (our unpublished results). Essentially identical surface transport kinetics was observed when cells were preincubated in the presence of bafilomycin A<sub>1</sub> to induce the complete collapse of MVT (Figure 9). An intact MVT is therefore not required for the surface transport of the major GPI-anchored glycoproteins, consistent with the notion that the MVT is not part of the normal exocytic pathway.

### *MVT Contains Resident Lysosomal Cysteine Proteases That Degrade pr-GFP In Vivo and In Vitro*

The subcellular fractionation studies suggested that the MVT contained mature cysteine proteases, although the activity of these proteases is insufficient to degrade the steady-state pool of pr-GFP. To investigate whether the slow rate of degradation of this protein was due to the relatively high pH of the MVT lumen, *L. mexicana* promastigotes were incubated in media adjusted to pH 5.5 for 2 h, conditions that are known to activate *Leishmania* cysteine proteases *in vitro* (Sanderson *et al.*, 2000). Although no detectable degradation of pr-GFP occurred when promastigotes were incubated in pH 7.5 medium, degradation of pr-GFP was essentially com-

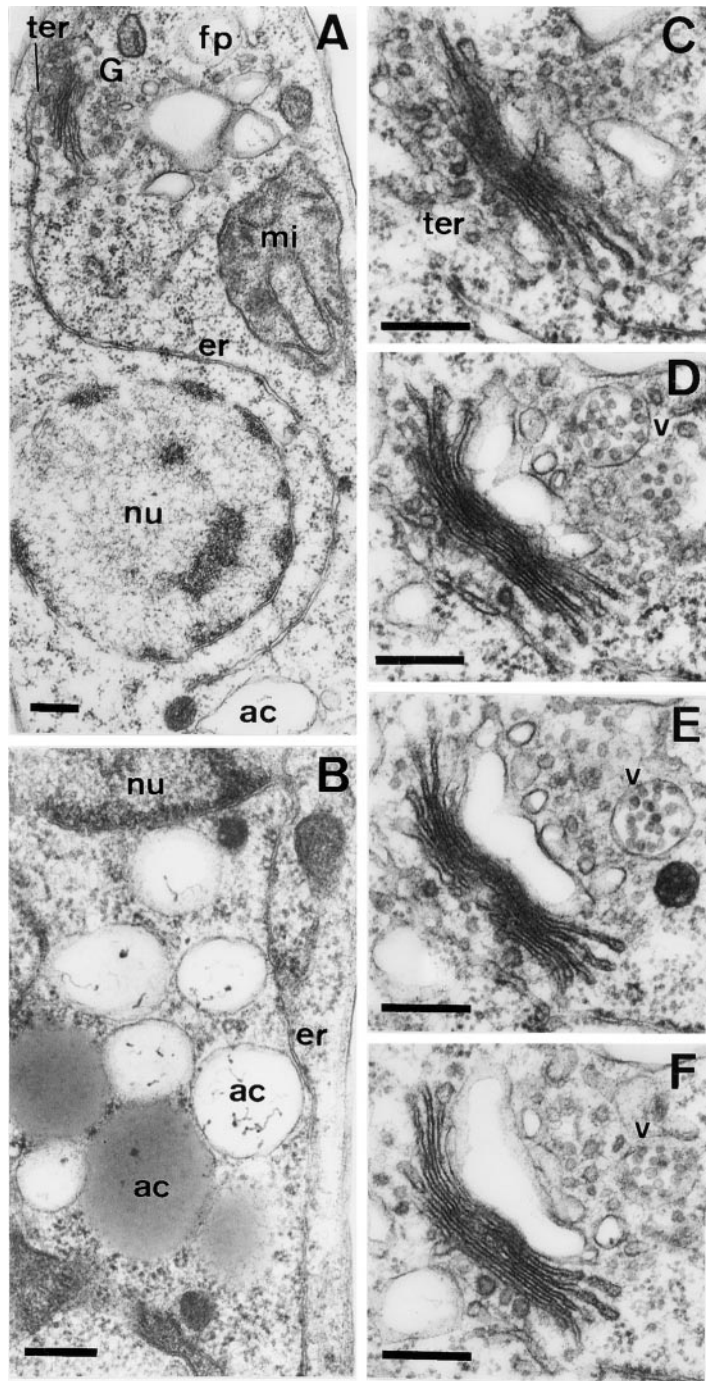


**Figure 7.** Multivesicular bodies are localized near the *trans*-face of the Golgi apparatus. (A) Overview of the anterior end of *L. mexicana* promastigotes (fixed in glutaraldehyde/osmium) showing that the transitional ER (ter) is formed from a cisternal extension of the cortical ER and is closely opposed to the *cis*-face of the single Golgi apparatus at the anterior end of the cell. (B) Detail of the posterior end of the cell, which is occupied by many acidocalcisomes (ac), a class of acidified, nonlytic vacuoles, which appear to be separate from the MVT. The original contents of these vacuoles are electron dense but can be extracted during the fixation. Note the continuation of nuclear envelope and ER. (C–F) Consecutive serial sections (one serial section has been left out between C and D) through a Golgi apparatus showing the tER-Golgi interface (ter), the Golgi stack (with 5–6 cisternae), and the active *trans*-face, which is associated with several types of vesicles, cisternal elements, and multivesicular bodies (MVB, v). Two MVBs can be seen in these consecutive sections. Abbreviations are as described in Figure 4. Bars, 250 nm.

plete after 2 h in pH 5.5 medium (Figure 10, compare lanes 1 and 4). In contrast, the ER pool containing the intact GFP-DPMS chimera was not degraded in either treatment (Figure 10). The degradation of pr-GFP at pH 5.5 was partially inhibited if the promastigotes were pretreated with E64d, a membrane-permeable inhibitor of the major lysosomal cysteine proteases of *Leishmania* (Figure 10, lane 2). Surprisingly, the serine protease inhibitor PMSF also retarded degradation of pr-GFP (Figure 10, lane 3). Similar

results were obtained when cells were incubated in the presence of cycloheximide (our unpublished results), indicating that the enhanced degradation at pH 5.5 did not reflect the inhibition of synthesis of new GFP-DPMS at the low pH or the increased synthesis of cysteine proteases. These results confirm the subcellular fractionation data showing that the MVT contains lysosomal cysteine proteinases and reveal the presence of a previously undescribed serine protease activity.

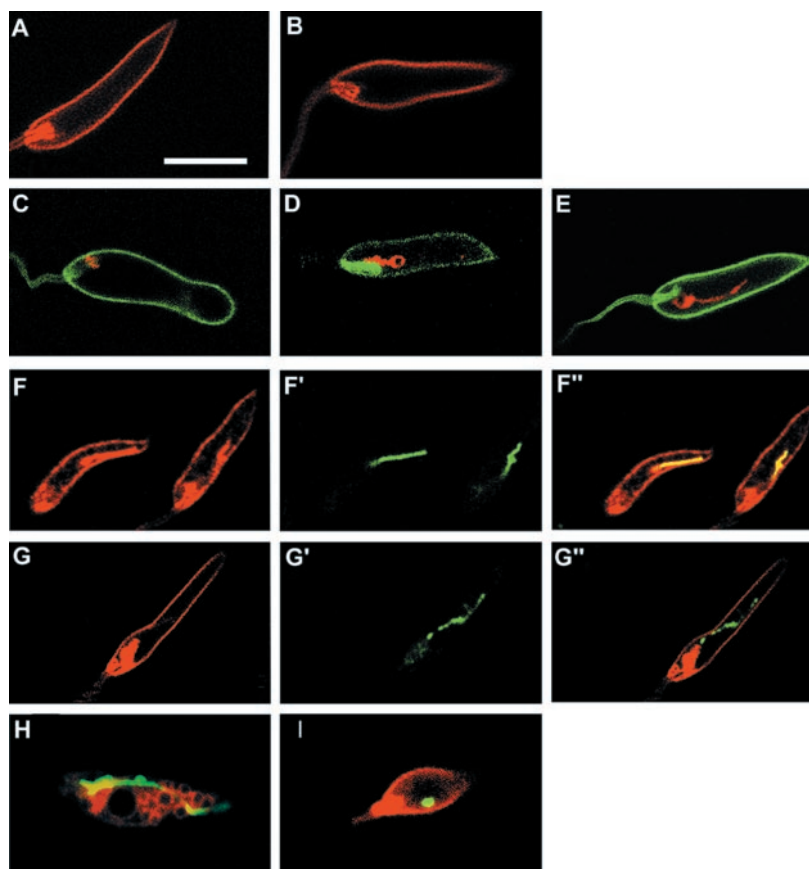


**Figure 8.** Uptake of FM 4-64 into the early endosomes and MVT. (A–E) Confocal microscopy of wild-type *L. mexicana* promastigotes labeled with FM 4-64. Promastigotes were labeled with FM 4-64 for 30 s at 27°C (A), or 2 h at 0°C (B) without back-extraction. Under these conditions, the FM 4-64 only labels the plasma membrane. Alternatively, promastigotes were labeled with FM 4-64 for 10 min and then incubated in fresh medium after back-extraction to remove the plasma membrane pool. After a 10-min (C), 20-min (D), or 2 h (E) chase, live promastigotes were surface labeled with concanavalin A-fluorescein isothiocyanate (green) to reveal the plasma membrane and flagellar pocket. FM 4-64 was first detected in endosomes near the flagellar pocket (C and D) before reaching the MVT (E). (F–G'') *L. mexicana* promastigotes expressing GFP-DPMS were labeled with FM 4-64 for 2 h at either 27°C (F–F'') or 10°C (G–G''). FM 4-64-labeled structures (F and G), GFP-labeled structures (F' and G'), and merged images (F'' and G''). (H) *L. mexicana* promastigotes expressing GFP-DPMS were stained with the acidotropic dye LysoTracker. LysoTracker was not present in the MVT but accumulates in the acidocalcisomes toward the posterior end of the cell (Figure 7B). When promastigotes expressing GFP-DPMS (I) were treated with bafilomycin A<sub>1</sub> (250 nM, 10 min), the MVT rapidly collapses to a single large vesicle. Bar, 5 μm.

The lytic capacity of the MVT, as judged by the rate of degradation of pr-GFP, was increased in stationary phase promastigotes (Figure 10, lanes 7–12). However, the degradation of pr-GFP at pH 5.5 was inhibited by E64d, but not by PMSF in these cells (Figure 10, lanes 7–9). These results are

consistent with previous reports that the proteolytic capacity of leishmanial lysosomes increases as promastigotes reach stationary growth (Mottram *et al.*, 1998; Rosenthal 1999), and further support the assignment of the MVT as a lysosomal compartment.

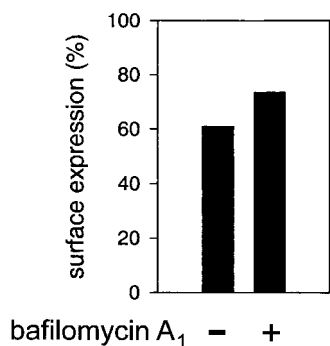


**Figure 9.** Perturbation of the MVT does not affect surface transport of the major surface glycoproteins. *L. mexicana* promastigotes were pulse-chase labeled with [<sup>35</sup>S]methionine and the surface transport of the major surface metalloproteinase gp63 measured by surface biotinylation after a 2-h chase. Cells were incubated in the absence or presence of 250 nM bafilomycin A<sub>1</sub> to vesicularize the MVT, before the labeling.

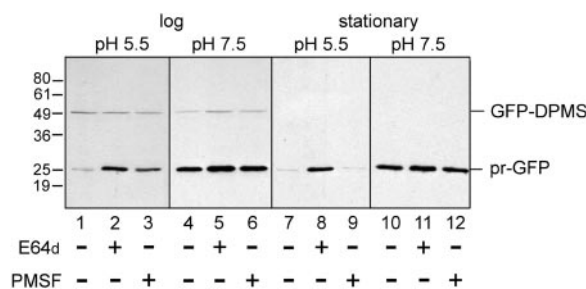


**Figure 10.** Degradation of GFP-DPMS is enhanced by acidification of the MVT and is developmentally regulated. Log or stationary phase promastigotes were suspended in pH 7.5 or 5.5 isotonic buffer and incubated for 2 h at 27°C in the absence (lanes 1, 4, 7, and 10) or presence of cysteine (lanes 2, 5, 8, and 11) or serine (lanes 3, 6, 9, and 12) protease inhibitors. These analyses are representative of four experiments. Similar results were obtained when cells were preincubated with cycloheximide.

## DISCUSSION

In this article we provide evidence that the ER glycosyltransferase DPMS is constitutively transported from a subcompartment of the ER to a novel tubular lysosome in *L. mexicana* promastigotes. Furthermore, we show that retention of GFP- and HA-tagged DPMS in the ER subcompartment is reduced as logarithmically growing *L. mexicana* promastigotes reach stationary growth, coincident with the down-regulation of DPMS activity in stationary phase cells. Soluble ER proteins are not transported to the lysosome or similarly degraded in stationary phase parasites, indicating that the degradation of DPMS is not the result of nonspecific turnover of ER membranes. Finally, we provide evidence that the elevated turnover of the DPMS chimeras in stationary phase promastigotes coincides with an increase in the lytic capacity of the MVT lysosome and changes in the morphology of this organelle. Collectively, these data suggest that growth-dependent changes in protein sorting to the lysosome may play an important role in regulating the cellular levels of DPMS and the biosynthesis of the major cell surface glycolipids of these parasites.

Our initial interest in the intracellular trafficking of DPMS arose from the finding that the GFP-DPMS chimera accumulated in a previously undescribed tubular compartment in *L. mexicana* promastigotes (Ilgoutz *et al.*, 1999b). This organelle is not induced by the overexpression of this protein because it is present in wild-type parasites labeled with the vital lipid stain BODIPY-ceramide (Ilgoutz *et al.*, 1999b) and the endocytic marker FM 4-64 (this study). The MVT can also be detected by EM in glutaraldehyde/osmium fixed (this study) and high-pressure frozen (Weise *et al.*, 2000) wild-type *L. mexicana* promastigotes. We now show that the MVT is a terminal lysosome compartment based on the following lines of evidence. First, the EM ultrastructural studies indicate that the MVT is a post-Golgi compartment with the same internal structure as late endosomes/lysosomes in other eukaryotic cells (Kobayashi *et al.*, 1998; Odorizzi *et al.*, 1998). Second, the MVT is labeled in a time- and temperature-dependent manner with the well-defined endocytic marker FM 4-64. These studies clearly show that the MVT is downstream of a network of tubulovesicular endosomes that surround the flagellar pocket. Transport between the endosomes and the MVT is specifically inhibited at 10°C, as previously reported for endosome-to-lysosome transport in the related parasite *Trypanosoma brucei* (Brickman *et al.*, 1995). FM 4-64 was not chased into other compartments, indicating that the MVT is the terminal compartment in the endosome/lysosomal pathway. The FM 4-64 studies also demonstrate that the MVT is distinct from the acidocalcisomes, a second class of acidified vacuoles in the parasites that contain the major cellular stores of Ca<sup>2+</sup> and polyphosphates (Docampo and Moreno, 1999). In contrast to the MVT, the acidocalcisomes were not labeled with FM 4-64. Third, with the use of subcellular fractionation we show that the MVT contains lysosomal cysteine proteases (Mottram *et al.*, 1998; Rosenthal, 1999). The activity of these proteinases is greatly enhanced if promastigotes are incubated in low pH medium, suggesting that the lytic capacity of the MVT may be regulated by changes in the luminal pH. The MVT of log phase promastigotes also appears to contain a previously uncharacterized serine protease activity. It is not known whether the serine protease activity occurs in stationary

phase cells as the activities of the cysteine proteases are highly up-regulated in this stage and are likely to mask other protease activities in these *in vivo* experiments. Fourth, the structure of the MVT is perturbed by a variety of lysomorphotropic compounds, including bafilomycin A<sub>1</sub>, monensin, and imipramine, which have been shown to affect lysosome function in other eukaryotes. Fifth, perturbation of the MVT does not alter the secretory transport of the metalloproteinase gp63, indicating that it is not part of the exocytic pathway used by the major surface GPI-anchored glycoproteins. These data are in agreement with a recent study of Overath and colleagues (Weise *et al.*, 2000) who concluded that the MVT is a post-Golgi compartment based on their EM ultrastructural analyses and the finding that the MVT contains complex phosphoglycans that are assembled in the Golgi apparatus.

Although the MVT appears to be the terminal compartment in the endocytic pathway of log phase promastigotes it has the characteristics of an immature lysosome. These include a low lytic capacity (as indicated by the accumulation of the pr-GFP and the abundant intraluminal vesicles) and a relatively high luminal pH (as indicated by the lack of staining with LysoTracker and the finding that exposure of parasites to low pH buffer greatly enhanced the degradation of the MVT localized pr-GFP). In contrast, the pr-GFP is rapidly degraded in stationary phase promastigotes, suggesting that the degradative capacity of this compartment increases dramatically in this stage. The mechanism(s) that underlie this maturation process have not been defined but may involve the increased synthesis of cysteine proteases (Mottram *et al.*, 1998; Rosenthal, 1999) as well as the acidification of the MVT lumen. The finding that the lytic capacity of the MVT is increased when the extracellular medium is acidified may be physiologically significant because *Leishmania* promastigotes are exposed to low pH when they invade mammalian macrophages and are internalized into the mature phagolysosomal compartment of the host cell. Low pH is thought to be one of the triggers for promastigote-to-amastigote differentiation, a process that involves the dramatic remodeling of secretory and endocytic organelles (Pimenta *et al.*, 1991). The rapid activation of parasite lysosomal hydrolases in response to low extracellular pH could be an important factor in initiating this remodeling process.

The MVT is closely associated with one or two specialized cytoplasmic microtubules that may facilitate the formation of this unusual organelle and the striking contraction and growth of the MVT during the cell cycle (Ilgoutz *et al.*, 1999b). These microtubules also appear to be invariably associated with the Golgi apparatus at the anterior end of the cell and become intercalated with the subpellicular array of microtubules that underlies the plasma membrane at the posterior end of the cell (cf. Weise *et al.*, 2000). Because microtubule-disrupting agents (Ilgoutz *et al.*, 1999b), as well as several lysomorphotropic compounds used in this study caused the MVT to collapse rapidly to a single large vesicle, we propose that the MVT is under elastic tension and that these microtubules may be involved in stabilizing this structure. They may also be involved in directing the transport of the MVBs to the anterior end of the MVT. At present it is not known whether these microtubules are continuous with the microtubule quartet that emerges from the flagellar basal body (Figure 6D; Gull, 1999) or to other microtubules that

may originate at the anterior end of the parasite (Weise *et al.*, 2000). In this respect, similar MVB- and MVT-like structures have been previously observed in *Crithidia fasciculata* and were proposed to associate with one (or two) microtubules in the flagellar pocket microtubule quartet that folded back into the cytoplasm before reaching the opening of the flagellar pocket (Brooker, 1971).

Our immuno-EM studies suggest that the GFP-DPMS chimera is transported to the MVT via the Golgi apparatus. Significantly, they also show that the GFP moiety is delivered to the lumen of the MVT consistent with the finding that this protein is rapidly degraded when promastigotes are incubated in low pH medium. In yeast and animal cells, many membrane proteins are targeted to the vacuole/lysosome lumen via the recently described MVB pathway (Hirst *et al.*, 1998; Kobayashi *et al.*, 1998; Odorizzi *et al.*, 1998). In this pathway, membrane proteins destined for lysosomal degradation are transported from either the Golgi apparatus or the plasma membrane to the limiting membrane of late endosomes and subsequently incorporated into microinvasinating vesicles that are released into the luminal compartment. After fusion of these MVBs with the vacuole/lysosome, the internal vesicles are delivered into the lysosome/vacuole lumen and degraded by luminal hydrolases (Odorizzi *et al.*, 1998). The presence of a similar pathway in *L. mexicana* promastigotes is strongly indicated by the presence of well-developed MVBs opposite the *trans*-Golgi apparatus (Figures 5 and 7). Whereas the location of the MVBs suggests that they arise from the Golgi apparatus, proteins and lipids could also be delivered to the MVBs via the endocytic pathway. Indeed, morphologically similar MVBs in *C. fasciculata* can be labeled with endocytic markers (Brooker, 1971) and several trypanosomatid lysosomal proteins are thought to be delivered to lysosomes via the endocytic pathway (Kelley *et al.*, 1995; Brooks *et al.*, 2000). Consistent with this possibility, some of the GFP chimera was localized to endosome membranes near the flagellar pocket (Figure 4). These observations suggest that the cytoplasmically orientated GFP-DPMS chimera may be transported from the ER to the Golgi apparatus and then delivered to the MVT lysosome via the MVB pathway from either the Golgi or endocytic pathway. It remains to be determined at what point in this pathway the GFP-DPMS chimera is initially cleaved. Because GFP fluorescence is never detected in the cytosol and cytosolic forms of GFP are not transported into the MVT (our unpublished data), it is unlikely that GFP-DPMS is cleaved before it has been internalized into the MVBs. Furthermore, a small steady-state pool of HA-DPMS was reproducibly detected in the dense MVT fractions (Figure 3B), suggesting that some of the membrane-bound DPMS reaches the MVT before it is degraded. It is also unknown how the size of the ER pool of DPMS is regulated during growth. Given that GFP-DPMS appears to be constitutively transported to the MVT in both log and stationary phase promastigotes the observed decrease in the size of the ER pool in stationary phase promastigotes could reflect a decrease in the capacity of ER retention and/or post-ER retrieval mechanism(s) in this stage.

Previous studies on the function of lysosomes in trypanosomatid parasites have focused on their role in nutrition and the degradation of surface-bound antibodies or other proteins involved in the host immune response (Overath *et al.*,

1997). The results of this study indicate that lysosomal degradation may have an important role in regulating the activity of some enzymes in the early secretory pathway of *L. mexicana*. The GFP-chimera proved to be useful for monitoring this process because the GFP moiety is remarkably stable and remains fluorescent after delivery to the MVT. These results are also of general interest because comparatively little is known about the role of lysosomal degradation in regulating the cellular levels of ER membrane proteins. In contrast, there is good evidence that the activities of several ER membrane proteins can be regulated by ubiquitination and the 26S proteasome system (Bonifacino and Weissman, 1998) or by endogenous ER proteases (Heinemann and Ozols, 1998). It will be of interest to determine whether these ER degradative pathways are also involved in regulating GPI biosynthetic enzymes in *Leishmania* spp.

## ACKNOWLEDGMENTS

We thank Dr. Ross Waller (University of Melbourne, Victoria, Australia) for generating the HA-tagged DPMS and for reading the manuscript, Dr. J.D. Bangs (University of Madison, Madison Medical School, Madison, WI) for providing the anti-BiP antibody, and Dr. J. Mottram (University of Glasgow, Glasgow, United Kingdom) for the anticysteine proteinase antibodies, and Professor Peter Overath (Max Planck Institute of Biology, Tübingen, Germany) for communicating results prior to publication. This work was supported by the Australian National Health and Medical Research Council and the Australian Research Council. M.J.M. is an Australian National Health and Medical Research Council Principal Research Fellow and Howard Hughes International Scholar. G.I.M. is a Howard Hughes International Scholar.

## REFERENCES

- Bangs, J.D., Uyetake, L., Brickman, M.J., Balber, A.E., and Boothroyd, J.C. (1993). Molecular cloning and cellular localization of a BiP homologue in *Trypanosoma brucei* - divergent ER retention signals in a lower eukaryote. *J. Cell Sci.* 10, 1101-1113.
- Bahr, V., Stierhof, Y.-D., Ilg, T., Demar, M., Quinten, M., and Overath, P. (1993). Expression of lipophosphoglycan, high molecular weight phosphoglycan and glycoprotein gp63 in promastigotes and amastigotes of *Leishmania mexicana*. *Mol. Biochem. Parasitol.* 58, 107-121.
- Bonifacino, J.S., and Weissman, A.M. (1998). Ubiquitin and control of protein fate in the secretory and endocytic pathways. *Annu. Rev. Cell Dev. Biol.* 14, 19-57.
- Bordier, C. (1981). Phase separation of integral membrane proteins in Triton X-114 solution. *J. Biol. Chem.* 256, 1604.
- Brickman, M.J., Cook, J.M., and Balber, A.E. (1995). Low temperature reversibly inhibits transport from tubular endosomes to a perinuclear, acidic compartment in African trypanosomes. *J. Cell Sci.* 108, 3611-3621.
- Brooker, B.E. (1971). The fine structure of *Crithidia fasciculata* with special reference to the organelles involved in the ingestion and digestion of protein. *Z. Zellforsch.* 11, 532-563.
- Brooks, D.R., Tetly, L., Coombs, G.H., and Mottram, J.C. (2000). Processing, and trafficking of cysteine proteases in *Leishmania mexicana*. *J. Cell Sci.* 113, 4035-4041.
- Docampo, R., and Moreno, S.N.J. (1999). Acidocalcisomes: a novel Ca<sup>2+</sup> storage compartment in trypanosomatids and apicomplexan parasites. *Parasitol. Today* 15, 443-448.

- Ferguson, M.A.J., Brimacombe, J.S., Brown, J.R., Crossman, A. Dix, A., Field, R.A., Guther, M.L.S., Milne, K.G., Sharma, D.K., and Smith, T.K. (1999). The GPI biosynthetic pathway as a therapeutic target for African sleeping sickness. *Biochim. Biophys. Acta* 1455, 327–340.
- Gruenberg, J., and Maxfield, F.R. (1995). Membrane transport in the endocytic pathway. *Curr. Biol.* 7, 552–563.
- Gull, K. (1999). The cytoskeleton of trypanosomatid parasites. *Annu. Rev. Microbiol.* 53, 629–655.
- Heinemann, F.S., and Ozols, J. (1998). Degradation of stearyl-coenzyme A desaturase: endoproteolytic cleavage by an integral membrane protease. *Mol. Biol. Cell* 9, 3445–3453.
- Hirst, J., Futter, C.E., and Hopkins, C.R. (1998). The kinetics of mannose 6-phosphate receptor trafficking in the endocytic pathway in Hep-2 cells: the receptor enters and rapidly leaves multivesicular endosomes without accumulating in the prelysosomal compartment. *Mol. Biol. Cell* 9, 809–816.
- Ilg, T. (2000). Lipophosphoglycan is not required for infection of macrophages or mice by *Leishmania mexicana*. *EMBO J.* 19, 1953–1962.
- Ilg, T., Handman, E., and Stierhof, Y.-D. (1999). Proteophosphoglycan from *Leishmania* promastigotes and amastigotes. *Biochem. Soc. Trans.* 27, 518–525.
- Ilgoutz, S.C., Mullin, K.A., Southwell, B.R., and McConville, M.J. (1999b). Glycosyl-phosphatidylinositol biosynthetic enzymes are localized to a stable tubular subcompartment of the endoplasmic reticulum in *Leishmania mexicana*. *EMBO J.* 18, 3643–3654.
- Ilgoutz, S.C., Zawadzki, J.L., Ralton, J.E., and McConville, M.J. (1999a). Evidence that free GPI glycolipids are essential for growth of *Leishmania mexicana*. *EMBO J.* 18, 2746–2755.
- Kelley, R.J., Brickman, M.J., and Balber, A.E. (1995). Processing and transport of a lysosomal membrane glycoprotein is developmentally regulated in African trypanosomes. *Mol. Biochem. Parasitol.* 74, 167–178.
- Kobayashi, T., Stang, E., Fang, K.S., de Moerloose, P., Parton, R.G., and Gruenberg, J. (1998). A lipid associated with the antiphospholipid syndrome regulates endosome structure and function. *Nature* 392, 193–197.
- Leidich, S.D., Drapp, D.A., and Orlean, P. (1994). A conditionally lethal yeast mutant blocked in the first step in glycosylphosphatidylinositol anchor synthesis. *J. Biol. Chem.* 269, 10193–10196.
- McConville, M.J., and Blackwell, J.M. (1991). Developmental changes in the glycosylated phosphatidylinositols of *Leishmania donovani*. Characterization of the promastigote and amastigote glycolipids. *J. Biol. Chem.* 266, 15170–15179.
- McConville, M.J., and Ferguson, M.A.J. (1993). The structure, biosynthesis and function of glycosylated phosphatidylinositol in the parasitic protozoa and higher eukaryotes. *Biochem. J.* 294, 305–324.
- McConville, M.J., and Menon, A.K. (2000). Recent developments in the cell biology and biochemistry of glycosylphosphatidylinositol lipids (review). *Mol. Membr. Biol.* 17, 1–16.
- Mengeling, B.J., Beverley, S.M., and Turco, S.J. (1997). Designing glycoconjugate biosynthesis for an insidious intent: phosphoglycan assembly in *Leishmania* parasites. *Glycobiology* 7, 873–880.
- Mottram, J.C., Brooks, D.R., and Coombs, G.H. (1998). Roles of cysteine proteinases of trypanosomes and *Leishmania* in host-parasite interactions. *Curr. Opin. Microbiol.* 1, 455–460.
- Mullin, K., Foth, B., Ilgoutz, S., Callaghan, J., and McConville, M. (2000). Characterization of a novel late endosome/lysosomal compartment in *Leishmania mexicana*. Molecular Parasitology Meeting XI, Marine Biological Laboratory, Woods Hole, MA.
- Nagamune, K., Nozaki, T., Maeda, Y., Ohishi, K., Fukuma, T., Hara, T., Schwartz, R.T., Sütterlin, C., Brun, R., Riezman, H., and Kinoshita, T. (2000). Critical roles of glycosyl-phosphatidylinositol for *Trypanosoma brucei*. *Proc. Natl. Acad. Sci. USA* 97, 10336–10341.
- Nozaki, M., Ohishi, K., Yamanda, N., Kinoshita, T., Nagy, A., and Takeda, J. (1999). Developmental abnormalities of glycosylphosphatidylinositol-anchor-deficient embryos revealed by Cre/loxP system. *Lab. Invest.* 79, 293–299.
- Odorizzi, G., Babst, M., and Emr, S.D. (1998). Fab1p PtdIns(3)P 5-kinase function essential for protein sorting in the multivesicular body. *Cell* 95, 847–858.
- Overath, P., Stierhof, Y.-D., and Weise, M. (1997). Endocytosis and secretion in trypanosomatid parasites -tumultuous traffic in a pocket. *Trends Cell Biol.* 7, 27–33.
- Pimenta, P.F., Saraiva, E.M., and Sacks, D.L. (1991). Comparative fine structure and surface glycosonjugate expression of three stages of *Leishmania major*. *Exp. Parasitol.* 72, 191–204.
- Ralton, J.E., and McConville, M.J. (1998). Delineation of three pathways of glycosylphosphatidylinositol biosynthesis in *Leishmania mexicana* - precursors from different pathways are assembled on distinct pools of phosphatidylinositol and undergo fatty acid remodeling. *J. Biol. Chem.* 273, 4245–4257.
- Rosenthal, P.J. (1999). Proteases of protozoan parasites. *Adv. Parasitol.* 43, 106–159.
- Sacks, D.L., Modi, G., Rowton, E., Spath, G., Epstein, L., Turco, S.J., and Beverley, S.M. (2000). The role of phosphoglycans in *Leishmania*-sand fly interactions. *Proc. Natl. Acad. Sci. USA* 97, 406–411.
- Sanderson, S.J., Pollock, K.G.J., Hilley, J.D., Meldal, M., St Hilaire, P., Juliano, M.A., Juliano, L., Mottram, J.C., and Coombs, G.H. (2000). Expression, and characterization of a recombinant cysteine proteinase of *Leishmania mexicana*. *Biochem. J.* 347, 383–388.
- Spath, G.F., Epstein, L., Leader, B., Singer, S.M., Avila, H.A., Turco, S.J., and Beverley, S.M. (2000). Lipophosphoglycan is a virulence factor distinct from related glycoconjugates in the protozoan parasite *Leishmania major*. *Proc. Natl. Acad. Sci. USA* 97, 9258–9263.
- Tiede, A., Bastisch, I., Schubert, J., Orlean, P., and Schmidt, R.E. (1999). Biosynthesis of glycosylphosphatidylinositols in mammals and unicellular microbes. *Biol. Chem.*, 380, 503–523.
- Travers, K.J., Patil, C.K., Wodicka, L., Lockart, D.J., Weissman, J.S., and Walter, P. (2000). Functional and genomic analyses reveal an essential coordination between the unfolded protein response and ER-associated degradation. *Cell* 101, 249–258.
- Udenfriend, S., and Kodukula, K. (1995). How glycosylphosphatidylinositol-anchored membrane proteins are made. *Annu. Rev. Biochem.* 64, 563–591.
- Vida, T.A., and Emr, S.D. (1995). A new vital stain for visualizing vacuolar membrane dynamics and endocytosis in yeast. *J. Cell Biol.* 128, 779–792.
- Wiese, M., Berger, O., Stierhof, Y.-D., Wolfram, M., Fuchs, M., and Overath, P. (1996). Gene cloning and cellular localization of a membrane-bound acid phosphatase of *Leishmania mexicana*. *Mol. Biochem. Parasitol.* 82, 153–165.
- Weise, F., Stierhof, Y.-D., Kühn, C., Wiese, M., and Overath, P. (2000). Distribution of GPI-anchored proteins in the protozoan parasite *Leishmania*, based on an improved ultrastructural description using high-pressure frozen cells. *J. Cell Sci.* 113, 4587–4603.
- Winter, G., Fuchs, M., McConville, M.J., Stierhof, Y.D., and Overath, P. (1994). Surface antigens of *Leishmania mexicana* amastigotes - characterization of glycoinositol phospholipids and a macrophage-derived glycosphingolipid. *J. Cell Sci.* 107, 2471–2482.